Chapter 5
Universal Representation of Dynamic Frequency Spectra for Canonical Generalised Quasicrystalline-Generated Waveguides

Z. Chen, A. K. M. Farhat, and M. Gei

Abstract An effective way to describe the sequence of stop and pass bands in a one-dimensional phononic waveguide is represented by the 'flow' line reported onto the plot of the relevant π-periodic reduced torus. In this chapter, these concepts are introduced for silver-mean quasicrystalline-generated elastic waveguides. Results are obtained for canonical configurations for which the dynamic frequency spectra are periodic. Application to finite-size waveguides is also illustrated. As the silver-mean sequence is one of the generalised Fibonacci sequences, the illustrated method can be easily extended to other quasicrystalline substitution rules.

5.1 Introduction

The study of elastodynamics of the class of two-phase periodic, one-dimensional waveguides whose elementary cells are generated through a quasicrystalline sequence has recently gained considerable attention. In a couple of early papers, Gei [1] and Morini and Gei [2] have provided the basic theory underlying the topic and introduced the fundamental tool of Kohmoto's invariant through which the main features of the problem can be explained: in particular, recursivity of traces of transmission matrices that govern the dynamic properties, self-similarity of the frequency spectra and the determination of the associated scaling factor, etc. The theory has been also applied to periodic media composed of laminae [3, 4] arranged according to the

Z. Chen · A. K. M. Farhat
School of Engineering, Cardiff University, The Parade, Cardiff CF24 3AA, U.K.
e-mail: chenz51@cardiff.ac.uk

A. K. M. Farhat
e-mail: farhatak@cardiff.ac.uk

M. Gei (✉)
Department of Engineering and Architecture, University of Trieste, via A. Valerio 6/1, 34127 Trieste, Italy
e-mail: massimiliano.gei@dia.units.it

Fibonacci chain (that is a quasicrystalline sequence), to show the capability of these composites to display negative refraction of antiplane shear waves.

Recently, Gei et al. [5] have defined the concept of *canonical* configurations for one-dimensional quasicrystalline-generated periodic waveguides for which, among several properties, the frequency spectra are periodic being the period a multiple of a particular frequency—the *canonical* frequency—that depends on the geometric and mechanical properties of the constituents of the elementary cell.

A further study [6] has shown how to employ the method of the dynamic flow on the *reduced torus*, proposed in elastodynamics by Shmuel and Band [7], to describe in an universal way the sequence of stop and pass bands for the same type of waveguides introduced in [1, 2]. A relevant application of this approach is that optimisation of the widths of stop bands becomes a simple graphical exercise when the reduced torus is adopted.

The goal of this note is to extend the latter concept to the case of silver-mean quasicrystalline-generated rods that are an example of waveguides obtained through a generalised Fibonacci sequence.

5.2 Wave Propagation in Silver-Mean Quasicrystalline Waveguides

We introduce a particular class of infinite, one-dimensional, two-component quasicrystalline phononic rods consisting of a repeated elementary cell in which two distinct phases, say L and S, are arranged according to the so-called *Silver-Mean* sequence, that is an example of *generalised Fibonacci* sequence. The repetition of the fundamental cell implies global periodicity along the axis and then the possibility of applying the Floquet-Bloch technique to investigate the propagation of harmonic elastic waves along the longitudinal axis of the rod. Each element of the class, denoted by $\mathscr{F}_i$ ($i = 0, 1, 2, \dots$), where the index i is the *order*, is constructed following the recursive rule

$$\mathscr{F}_i = \mathscr{F}_{i-1}^2 \mathscr{F}_{i-2}, \tag{5.1}$$

where the initial condition is $\mathscr{F}_0 = S$ and $\mathscr{F}_1 = L$ (in Fig. 5.1, elementary cells representing $\mathscr{F}_2$, $\mathscr{F}_3$ and $\mathscr{F}_4$ are sketched). Each cell $\mathscr{F}_i$ is composed of $\tilde{n}_i$ elements, where $\tilde{n}_i = 2\tilde{n}_{i-1} + \tilde{n}_{i-2}$ ($i \geq 2$) and $\tilde{n}_0 = \tilde{n}_1 = 1$. The limit $\tilde{n}_{i+1}/\tilde{n}_i$ for $i \to \infty$ corresponds to the *silver-mean ratio* $(1 + \sqrt{2}) \cong 2.414$.[1]

Consider now the geometrical and physical properties of phases L and S. The lengths of the two elements are indicated, respectively, with l_L and l_S, while A_J, E_J and ϱ_J ($J \in \{L, S\}$ here and henceforth) denote cross-section area, Young's modulus and mass density per unit volume of each element, respectively. For both

[1] In general, all sequences that follow the rule $\mathscr{F}_i = \mathscr{F}_{i-1}^m \mathscr{F}_{i-2}$ ($m \geq 1$) are quasicrystalline; see the discussion in [2].

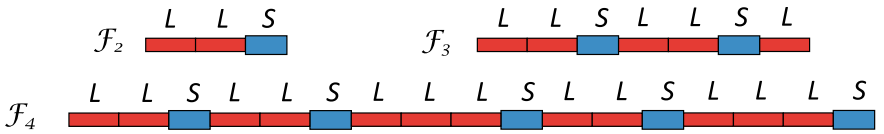

Fig. 5.1 Sketch of elementary cells for silver-mean phononic rods whose elements of the sequence are $\mathscr{F}_2$, $\mathscr{F}_3$ and $\mathscr{F}_4$

segments, we define the displacement function along the rod $u(z)$ and the axial force $N(z) = EAu'(z)$, where z is the longitudinal coordinate. The governing equation of longitudinal harmonic axial waves in each phase is

$$u''_J(z) + Q_J\,\omega^2 u_J(z) = 0, \tag{5.2}$$

where ω is the circular frequency and $Q_J = \varrho_J/E_J$. The general solution to Eq. (5.2) is

$$u_J(z) = C_J \sin(\sqrt{Q_J}\,\omega z) + D_J \cos(\sqrt{Q_J}\,\omega z), \tag{5.3}$$

where C_J and D_J are constants.

To obtain the dispersion diagram of the periodic rod, displacement and axial force at the right-hand boundary of the elementary cell, respectively, u_r and N_r, have to be identified in terms of those at the left-hand boundary, respectively, u_l and N_l, as

$$\boldsymbol{U}_r = \boldsymbol{T}_i \boldsymbol{U}_l, \tag{5.4}$$

where $\boldsymbol{U}_j = [u_j\ N_j]^T$ $(j = r, l)$ and $\boldsymbol{T}_i$ is the 2×2 transmission matrix of the cell $\mathscr{F}_i$. The latter is the result of the product $\boldsymbol{T}_i = \prod_{p=1}^{\tilde{n}_i} \boldsymbol{T}^J$, where $\boldsymbol{T}^J$ is the transmission matrix relating quantities across a single element that can be found explicitly in [2]. $\boldsymbol{T}_i$ is unimodular ($\det \boldsymbol{T}_i = 1$) and follows, from Eq. (5.1), the recursion rule $\boldsymbol{T}_{i+1} = \boldsymbol{T}_{i-1}\boldsymbol{T}_i^2$ $(i > 0)$, with $\boldsymbol{T}_0 = \boldsymbol{T}^S$ and $\boldsymbol{T}_1 = \boldsymbol{T}^L$.

Periodicity allows the Floquet-Bloch condition to be applied to the problem, namely $\boldsymbol{U}_r = \exp(\mathrm{i}K)\boldsymbol{U}_l$, so that, by combining this with Eq. (5.4), the dispersion equation

$$\cos K = x_i/2 \tag{5.5}$$

is achieved, where $x_i = \mathrm{tr}\boldsymbol{T}_i$. The solution to Eq. (5.5) provides the complete Floquet-Bloch spectrum and allows the definition stop-/pass-band pattern of each waveguide at varying index i. Waves propagate when $|x_i| < 2$, stop bands correspond to the ranges of frequencies where $|x_i| > 2$, whereas $|x_i| = 2$ characterises standing waves.

5.3 Universal Representation of the Frequency Spectrum

To achieve the goal of this article, it is instrumental to introduce the following functions of the circular frequency ω, i.e.

$$\zeta_S(\omega) = l_S\sqrt{Q_S}\omega, \quad \zeta_L(\omega) = l_L\sqrt{Q_L}\omega. \tag{5.6}$$

General recursive relations for the traces of unimodular transfer matrices of generalised Fibonacci chains have been derived in terms of Chebyshev polynomials of the first and second kind. Specialising these expressions to the silver-mean case, it turns out that

$$\begin{cases} x_i = x_{i-1}t_i - x_{i-2}, \\ t_{i+1} = x_i x_{i-1} - t_i, \end{cases} \quad (i \geq 2), \tag{5.7}$$

where $t_i = \mathsf{tr}(\boldsymbol{T}_{i-2}\boldsymbol{T}_{i-1})$. Through the new set of variables

$$\tilde{x}_i = t_{i+2}, \ \tilde{y}_i = x_{i+1}, \ \tilde{z}_i = x_i \tag{5.8}$$

and its substitution into expression (5.7), the following nonlinear discrete map determining the evolution of x_i and t_i is obtained

$$\mathscr{T} : \mathbb{R}^3 \to \mathbb{R}^3, \ \mathscr{T}(\tilde{x}_i, \tilde{y}_i, \tilde{z}_i) = (\tilde{x}_{i+1}, \tilde{y}_{i+1}, \tilde{z}_{i+1}) = \big(\tilde{x}_i\tilde{y}_i^2 - \tilde{y}_i\tilde{z}_i - \tilde{x}_i, \ \tilde{x}_i\tilde{y}_i - \tilde{z}_i, \ \tilde{y}_i\big), \tag{5.9}$$

where the initial conditions are given by

$$\tilde{z}_0 = x_0 = 2\cos\zeta_S, \quad \tilde{y}_0 = x_1 = 2\cos\zeta_L, \quad \tilde{x}_0 = t_2 = 2\cos\zeta_L\cos\zeta_S - \beta\sin\zeta_L\sin\zeta_S. \tag{5.10}$$

In Eq. (5.10), the impedance mismatch β takes the form

$$\beta = \frac{A_L^2E_L^2Q_L + A_S^2E_S^2Q_S}{A_LE_LA_SE_S\sqrt{Q_LQ_S}}. \tag{5.11}$$

The generic trace x_i can be derived through successive iterations of the expressions in Eq. (5.7) by assuming (5.10) as initial conditions[2] which include 2π-periodic functions of their arguments. Therefore, x_i is also a 2π-periodic function of both ζ_L and ζ_S as it is defined through sums and products of functions with the same period. This implies that we can consider each x_i as a function of a two-dimensional torus of edge length 2π, whose toroidal and poloidal coordinates correspond to ζ_S and ζ_L, respectively. More in detail, the toroidal domain, independent of l_L and l_S, is composed of two complementary subspaces that are associated with $|x_i(\zeta_S, \zeta_L)| < 2$ (pass band) and $|x_i(\zeta_S, \zeta_L)| > 2$ (stop band). The two regions are separated by lines in

[2] For instance, it turns out that $x_2 = 2\cos(2\zeta_L)\cos(\zeta_S) - \beta\sin(2\zeta_L)\sin(\zeta_S)$.

which $|x_i(\zeta_S, \zeta_L)| = 2$ (standing-wave solution). The measures of the two subregions are univocally determined by the value of β.

Equation (5.5) shows that $|x_i(\zeta_S, \zeta_L)|$ is invariant under the transformation

$$\zeta_S \to \zeta_S + n\pi, \quad \zeta_L \to \zeta_L + m\pi \quad (n, m \in \mathbb{N}), \tag{5.12}$$

so that the map on the torus can be equivalently represented on a reduced π-periodic torus (the *reduced torus*) that is a—flat—square whose edges are still described by coordinates ζ_S and ζ_L, both ranging now between 0 and π.

Examples of stop- and pass-band domains within the corresponding reduced tori are displayed, for $\beta = 2.5$, in Figs. 5.2, 5.3 and 5.5 for cells $\mathscr{F}_2$, $\mathscr{F}_3$ and $\mathscr{F}_4$, respectively, in particular stop-band regions are coloured in light blue.

The sequence of stop bands and pass bands of a silver-mean waveguide of any arbitrary order can be studied by analysing the linear 'flow' parametrised by map $(\zeta_S(\omega), \zeta_L(\omega))$ on the reduced torus, where ω is the time-like parameter. Note that in this parametrisation the lengths of the two phases come into play and contribute to the inclination of the trajectory together with quantities $\sqrt{Q_J}$. Thanks to conditions (5.12), the 'flow' lines are subdivided into ordered sequences of segments within the reduced torus. The starting point of a segment depends on the final point of the previous one. As $\omega > 0$, the initial point of each trajectory is the origin. Two examples of trajectory are the black lines sketched in Figs. 5.2 and 5.3. However, an additional piece of theory is required to fully capture the information conveyed by the plots.

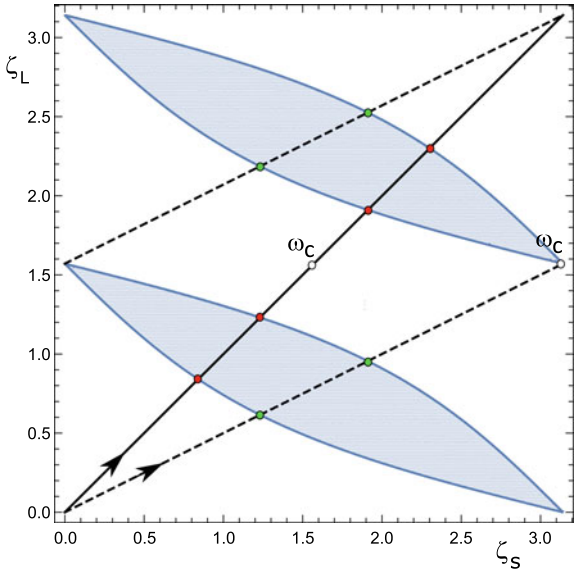

Fig. 5.2 Flow lines on the reduced torus for a canonical silver-mean phononic rod whose elementary cell is $\mathscr{F}_2$ and $\beta = 2.5$. Solid line: $l_S/l_L = 1,\ A_S/A_L = 1/2,\ Q_S/Q_L = 1$ ($\mathscr{C}_1 = 1$); dashed line: $l_S/l_L = 2,\ A_S/A_L = 1/2,\ Q_S/Q_L = 1$ ($\mathscr{C}_3 = 2$). Coloured dots mark the extremes of the stop bands

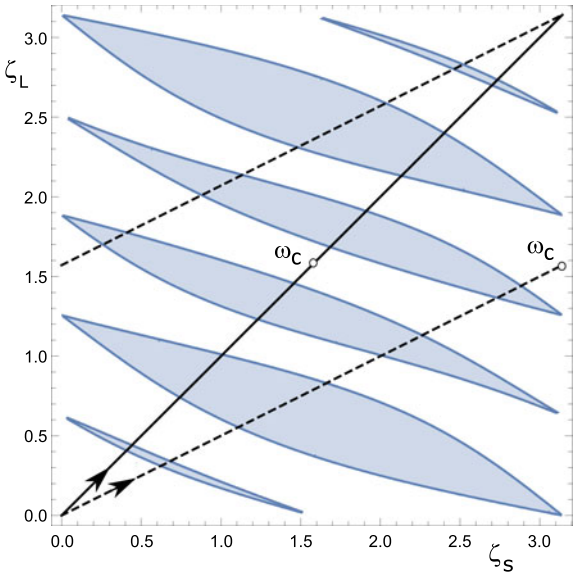

Fig. 5.3 Flow lines on the reduced torus for a canonical silver-mean phononic rod whose elementary cell is $\mathscr{F}_3$ and $\beta = 2.5$. Solid line: $l_S/l_L = 1,\ A_S/A_L = 1/2,\ Q_S/Q_L = 1$ ($\mathscr{C}_1 = 1$); dashed line: $l_S/l_L = 2,\ A_S/A_L = 1/2,\ Q_S/Q_L = 1$ ($\mathscr{C}_3 = 2$)

5.4 Canonical Configurations

In [8], the notions of *canonical configuration* and *canonical frequency* for silver-mean periodic waveguides have been proposed. For the problem analysed in this note, the most important feature of a canonical waveguide is that the frequency spectrum is *periodic*, and the period of the sequence of stop and pass bands matches twice the canonical frequency ($\omega_{\mathscr{C}}$ from now on).

A silver-mean canonical waveguide is such when the ratio $\mathscr{C} = l_S/l_L\sqrt{Q_S/Q_L}$ is a rational number, namely

$$\mathscr{C}_1 = \frac{1+2j}{1+2k} \quad \text{or} \quad \mathscr{C}_2 = \frac{1+2j}{2q} \quad \text{or} \quad \mathscr{C}_3 = \frac{2q}{1+2k} \quad (j,k \in \mathbb{N}, q \in \mathbb{N}^+) \tag{5.13}$$

where the separation in three distinct ratios (or families) comes from the detailed analysis reported in [8]. We note that family no. 1 encompasses odd/odd ratios, while odd/even and even/odd ratios are associated with family nos. 2 and 3, respectively, and it is important to remark that indices j, k and q in (5.13) are such that fractions on the right-hand sides are in the lowest terms.

The corresponding canonical frequencies are

$$\omega_{\mathscr{C}_1} = \omega_{\mathscr{C}_3} = \frac{\pi}{2l_L\sqrt{Q_L}}(1+2k), \quad \omega_{\mathscr{C}_2} = \frac{\pi}{l_L\sqrt{Q_L}}q \quad (k \in \mathbb{N}, q \in \mathbb{N}^+), \tag{5.14}$$

where k, q coincide with the analogous indices selected in the relevant condition among those listed in (5.13).

The periodicity of the frequency spectrum of canonical waveguides is evident on the reduced torus as the trajectory becomes, in turn, periodic. This means that at $\omega = 2\omega_{\mathscr{C}}$ the point of the 'flow' coincides with that of coordinate (π, π) and for $\omega > 2\omega_{\mathscr{C}}$ the trajectory repeats itself starting from the origin. This occurs each time a frequency multiple of $2\omega_{\mathscr{C}}$ is reached.

5.5 Results

The reduced torus in Fig. 5.2 is for an elementary cell constructed adopting $\mathscr{F}_2$ and for the set of parameters $A_S/A_L = 1/2,\ E_S/E_L = 1,\ Q_S/Q_L = 1$; therefore, the impedance mismatch parameter is $\beta = 2.5$. Two flow lines are sketched—in black—namely, the solid one is for $l_S/l_L = 1$ whereas the dashed one describes the ratio $l_S/l_L = 2$; therefore, the former associated rod belongs to the first family of canonical waveguides (cfr. (5.13)) being $\mathscr{C}_1 = 1$ ($j = k = 0$), whereas the latter belongs to the third family ($\mathscr{C}_3 = 2, q = 1,\ k = 0$).

The solid line is the diagonal of the square (reduced torus) and represents the whole trajectory for the former structure in the interval $\omega \in [0, 2\omega_{\mathscr{C}}]$ (here $l_L\sqrt{Q_L}\omega_{\mathscr{C}} = \pi/2$); hence, for frequencies just greater than the threshold $2\omega_{\mathscr{C}}$, the trajectory runs along the same segment re-starting from the origin. For the latter canonical configuration, the trajectory in the period $[0, 2\omega_{\mathscr{C}}]$ is composed of two segments (dashed) (where, again, $l_L\sqrt{Q_L}\omega_{\mathscr{C}} = \pi/2$). In both cases, the point at which $\omega = \omega_{\mathscr{C}}$ is depicted with a white circle.

For both cases, when at a given frequency the point of the flow lies in the white region, the frequency itself sits in a pass band; conversely, when the point is in the light-blue domain, the frequency is in a stop band. The limit of the stop bands is marked with coloured dots.

Figure 5.3 reports the same information (all parameters match those of the previous figure), but the reduced torus is for an elementary cell $\mathscr{F}_3$. It is clear now that the distribution of stop and pass bands is remarkably different as the light-blue subregions are in a greater number with respect to that in Fig. 5.2. This makes more involved the computation of the number of stop bands for any canonical configuration associated with the same value of β; however, the reduced torus proved to be an exceptional tool to understand how the sequence of stop and pass bands evolves for a given canonical configuration in a period. As a further example showing the increasing complexity for high-order elementary cells, the reduced torus for $\mathscr{F}_4$ is sketched in Fig. 5.5.

In order to give the reader an additional insight into the diagrams illustrated in Figs. 5.2 and 5.3, we consider two finite waveguides composed of six elementary cells $\mathscr{F}_2$ and $\mathscr{F}_3$, respectively. They join two semi-infinite, identical outer media whose elastic properties match those of phase L (the common schematic is depicted in Fig. 5.4a)). We expect the system to be able to transmit (resp. reflect) a signal whose frequency belongs to a pass band (resp. stop band). To this end, transmission coefficient T_c and reflection coefficient $R_c = 1 - T_c$ can be calculated following the method presented in [9]. The reflection coefficients for the two problems at hand

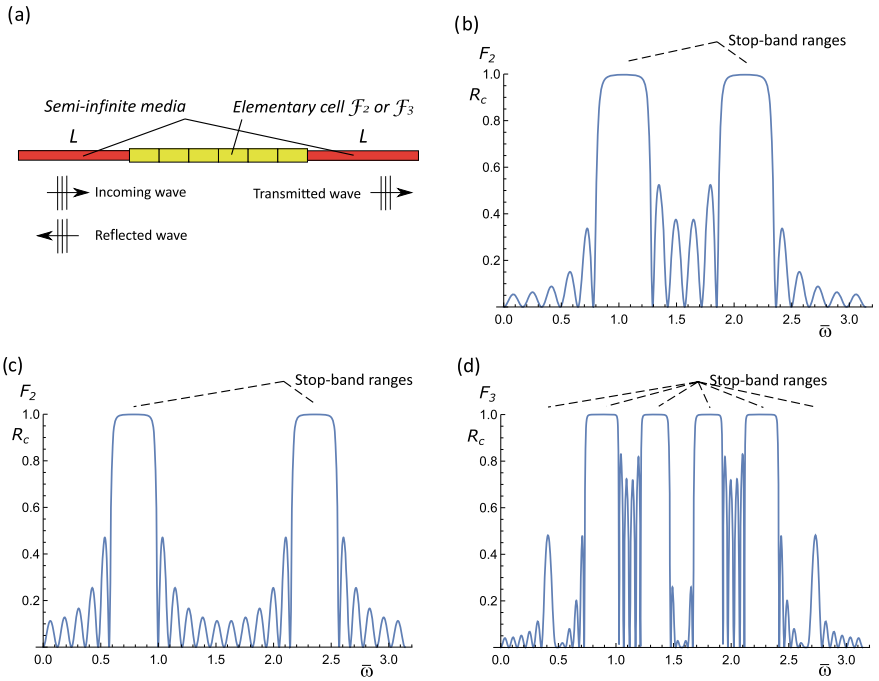

Fig. 5.4 Reflection of axial waves in a finite-sized silver-mean phononic waveguide ($\beta = 2.5$ in all analysed cases): **a** schematic of the device; **b** plot of the reflection coefficient R_c for elementary cell $\mathscr{F}_2$ ($l_S/l_L = 1,\ A_S/A_L = 1/2,\ Q_S/Q_L = 1, \mathscr{C}_1 = 1$) for a dimensionless frequency in the interval $[0, 2\,l_L\sqrt{Q_L}\omega_{\mathscr{C}}\,]$; **c** plot of R_c for elementary cell $\mathscr{F}_2$ ($l_S/l_L = 2,\ A_S/A_L = 1/2,\ Q_S/Q_L = 1, \mathscr{C}_3 = 2$) in the interval $[0, 2\,l_L\sqrt{Q_L}\omega_{\mathscr{C}}\,]$; **d** plot of R_c for elementary cell $\mathscr{F}_3$ ($l_S/l_L = 1,\ A_S/A_L = 1/2,\ Q_S/Q_L = 1, \mathscr{C}_1 = 1$) in the interval $[0, 2\,l_L\sqrt{Q_L}\omega_{\mathscr{C}}\,]$

are displayed in Fig. 5.4. On the one hand, for cell $\mathscr{F}_2$, the whole—dimensionless—frequency domain $[0, 2\,l_L\sqrt{Q_L}\,\omega_{\mathscr{C}}\,]$ represented in Fig. 5.2 is analysed in Fig. 5.4b and c for the two length ratii. On the other hand, Fig. 5.4d describes the case of cell $\mathscr{F}_3$ (Fig. 5.3) with $l_S/l_L = 2$. Note that the two peaks in Fig. 5.4c are more distant from each other than those in Fig. 5.4b and this is consistent with the information obtained following the two flow lines in Fig. 5.2.

In all diagrams, it is evident that R_c approaches 1 (i.e. total reflection) in the frequency ranges that correspond to stop bands, thus confirming that the model of infinite, periodic waveguide provides an excellent estimation of frequencies at which waves cannot propagate. Only for the two outer stop bands of Fig. 5.4d the match is not very good because six cells in the finite-size waveguide are not enough as it is well known that narrow stop bands require a high number of elements to be correctly captured by such a waveguide. For the same reason, the function $R_c(\omega)$ is oscillatory and not null in the corresponding pass bands.

In closing the section, a natural question may arise when thinking about the reduced-torus representation: what is the key information conveyed by the white and

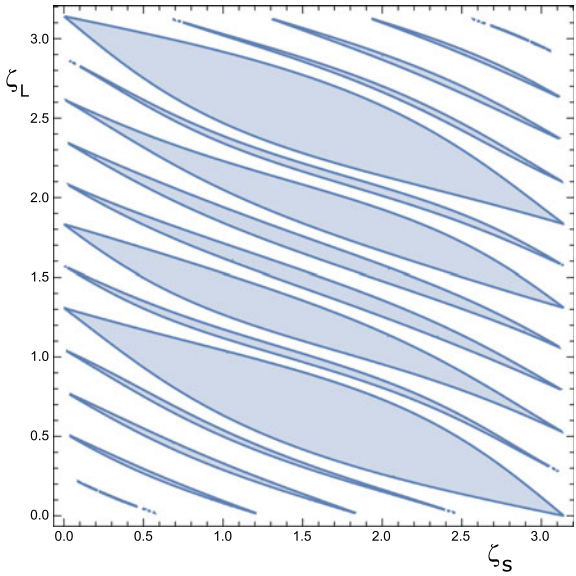

Fig. 5.5 Reduced torus for a canonical silver-mean phononic rod whose elementary cell is $\mathscr{F}_4$ and $\beta = 2.5$

light-blue regions in the square when the structure is 'non-canonical', namely when $\mathscr{C}$ is irrational? In this case, the spectrum is not periodic, the flow lines are 'open' and cover ergodically the whole square at increasing frequency. Consequently, the flow trajectories on the torus consist of an infinite number of parallel segments which, in turn, cover the whole square domain. Therefore, for the frequency spectrum, we can define the 'stop-band density' that is given by the ratio between the area of the light-blue subdomain and that of the square, i.e. π^2. Since the measure of stop-band domain is determined only by the parameter β, which is independent of the ratio l_S/l_L, for non-canonical bars the stop-band density does not depend on the ratio between lengths of the phases (Fig. 5.5).

5.6 Conclusions

Through the adoption of the silver-mean Fibonacci sequence, we have extended to generalised quasicrystalline-generated waveguides the method to represent the layout of stop and pass bands by flow lines on the square domain of the reduced torus. The reduced torus is an effective graphical way to display pass-band and stop-band regions for a set of configurations sharing the same impedance mismatch parameter. Specific results reported in the note are given for canonical configurations, for which the frequency spectra are periodic; as a consequence, the relevant trajectories on the reduced torus at varying frequencies are periodic and are composed of a finite number of segments. For non-canonical configurations, the trajectories cover ergodically the

whole domain and it can be shown that the stop-band density does not depend on the ratio between lengths of the phases. Finite-size waveguides are also studied and the values of the reflection coefficient confirm the reliability of the Floquet-Bloch method. The tool of the reduced torus can be profitably employed for optimisation problems such as maximisation of the widths of stop bands.

Acknowledgements ZC acknowledges support from China Scholarship Council (grant no. CSC201908500111). AKMF acknowledges support from the Embassy of Lybia (ref. no. 13556). MG is grateful for the support provided by Fondazione Cassa di Risparmio di Gorizia.

References

1. Gei M (2010) Int J Solids Struct 47:3067
2. Morini L, Gei M (2018) J Mech Phys Solids 119:83
3. Morini L, Eyzat Y, Gei M (2019) J Mech Phys Solids 124:282
4. Chen Z, Morini L, Gei M (2022) Phil Trans R Soc A, art n 20210401
5. Gei M, Chen Z, Bosi F, Morini L (2020) Appl Phys Lett 116, art n 241903
6. Morini L, Tetik ZG, Shmuel G, Gei M (2019) Phil Trans R Soc A 378, art n 20190240
7. Shmuel G, Band R (2016) J Mech Phys Solids 92:127
8. Farhat AKM, Morini L, Gei M (2022) J Sound Vib 553, art n 116679
9. Lekner J (1994) J Opt Soc Am A 11:2892